Title

Serum MicroRNA Transcriptomics and Acute Rejection or Recurrent Hepatitis C Virus in Human Liver Allograft Recipients: A Pilot Study

Journal

Transplantation, 106(4)

ISSN

0041-1337

Authors

Muthukumar, Thangamani
Akat, Kemal M
Yang, Hua
et al.

Publication Date

2022-04-01

DOI

10.1097/tp.0000000000003815

Peer reviewed

HHS Public Access

Author manuscript

Transplantation. Author manuscript; available in PMC 2023 April 01.

Published in final edited form as:

Transplantation. 2022 April 01; 106(4): 806–820. doi:10.1097/TP.0000000000003815.

Serum MicroRNA Transcriptomics and Acute Rejection or Recurrent Hepatitis C Virus in Human Liver Allograft Recipients: A Pilot Study

Thangamani Muthukumar, MD[#1], **Kemal M. Akat, MD**[#2,#], **Hua Yang, MD**[#1], **Joseph E. Schwartz, PhD**[1,3], **Carol Li, BS**[1], **Heejung Bang, PhD**[4], **Iddo Z. Ben-Dov, MD, PhD**[2], **John R. Lee, MD**[1], **David Ikle, PhD**[5], **Anthony J. Demetris, MD**[6], **Thomas Tuschl, PhD**[2], **Manikkam Suthanthiran, MD**[1]

[1]Division of Nephrology and Hypertension, Joan and Sanford I. Weill Department of Medicine and Department of Transplantation Medicine, New York Presbyterian-Weill Cornell Medicine, New York, NY.

[2]Laboratory of RNA Molecular Biology, The Rockefeller University, New York, NY.

[3]Department of Psychiatry and Behavioral Science, Stony Brook University, Stony Brook, NY.

[4]Division of Biostatistics, Department of Public Health Sciences, University of California at Davis, Davis, CA.

[5]Rho Federal Systems, Chapel Hill, NC.

[6]Division of Transplantation Pathology, Department of Pathology, University of Pittsburgh Medical Center, Pittsburgh, PA.

[#] These authors contributed equally to this work.

Abstract

Background.—Acute rejection (AR) and recurrent HCV (R-HCV) are significant complications in liver allograft recipients. Noninvasive diagnosis of intragraft pathologies may improve their management.

Methods.—We performed small RNA sequencing and miRNA microarray profiling of RNA from sera matched to liver allograft biopsies from patients with nonimmune, nonviral (NINV) native liver disease. Absolute levels of informative miRNAs in 91 sera matched to 91 liver allograft biopsies were quantified using customized RT-qPCR assays: 30 biopsy-matched sera

Correspondence Information: Thomas Tuschl, PhD, Laboratory of RNA Molecular Biology, The Rockefeller University, 1230 York Avenue, New York, NY 10065. ttuschl@rockefeller.edu, Manikkam Suthanthiran, MD, Division of Nephrology and Hypertension, New York Presbyterian-Weill Cornell Medicine, Box 3, 525 E 68 Street, New York, NY 10065. msuthan@med.cornell.edu.

Authorship

T.M., K.M.A., H.Y., T.T., and M.S. designed research.
T.M., K.M.A., H.Y., and C.L. performed research.
T.M., K.M.A., H.Y., J.E.S., H.B., I.Z.B.-D., D.I., A.J.D., T.T., and M.S. analyzed data.
T.M., K.M.A., H.Y., J.E.S., J.R.L., T.T., and M.S. wrote the paper.

[#]Current address: Division of Cardiovascular Medicine, Vanderbilt University Medical Center, Nashville, TN.

Disclosure

The other authors of this manuscript declare no conflicts of interest. The other authors have no disclosures.

from 26 unique NINV patients and 61 biopsy-matched sera from 41 unique R-HCV patients. The association between biopsy diagnosis and miRNA abundance was analyzed by logistic regression and calculating the area under the receiver operating characteristic curve.

Results.—Nine miRNAs- miR-22, miR-34a, miR-122, miR-148a, miR-192, miR-193b, miR-194, miR-210 and miR-885–5p- were identified by both sRNA-seq and TLDA to be associated with NINV-AR. Logistic regression analysis of absolute levels of miRNAs and goodness-of-fit of predictors identified a linear combination of miR-34a + miR-210 ($P<0.0001$) as the best statistical model and miR-122 + miR-210 ($P<0.0001$) as the best model that included miR-122. A different linear combination of miR-34a + miR-210 ($P<0.0001$) was the best model for discriminating NINV-AR from R-HCV with intragraft inflammation, and miR-34a + miR-122 ($P<0.0001$) was the best model for discriminating NINV-AR from R-HCV with intragraft fibrosis.

Conclusions.—Circulating levels of miRNAs, quantified using customized RT-qPCR assays, may offer a rapid and noninvasive means of diagnosing AR in human liver allografts and for discriminating AR from intragraft inflammation or fibrosis due to recurrent HCV.

ClinicalTrials.gov identifier: NCT01428700

INTRODUCTION

Liver transplantation is the second most common type of solid organ transplantation in the United States, with 8250 liver transplants performed in 2018. This reflects an increase compared to 2017 and includes deceased donor and living donor allografts and adult, pediatric, repeat and multiorgan transplants.[1]

About 12% of all liver allograft recipients, and about 20% of recipients aged 18–34, experience an acute rejection within the first 12 months of transplantation despite the multi-drug armamentarium available to transplant clinicians.[1] Maintenance immunosuppressive drug therapy is also associated with multiple complications. A major goal is to minimize drug therapy without risking rejection.[2–4]

The diagnosis of acute liver allograft rejection is confirmed by liver allograft biopsy findings.[5] The biopsy procedure has become safer and the biopsy readings more standardized over the years but this invasive procedure is still associated with complications.[6–8] Moreover, anti-allograft immune responses are dynamic and repeat biopsies to monitor the kinetics pose safety concerns and additional costs. Development of noninvasive biomarkers diagnostic of rejection could allay some of these concerns and be of value for monitoring immunosuppression minimization.[9]

MicroRNAs (miRNA) are a class of small noncoding RNAs, 19 to 24 nucleotides in length. miRNA regulate gene expression by mRNA cleavage and by translational repression.[10] An individual miRNA's ability to regulate expression of multiple immune genes have led to their recognition as key regulators of immunity including anti-allograft immunity.[11,12] Existing literature also support miRNAs as biomarkers of disease ranging from malignancies to rejection in human allografts.[13–19]

Small RNA sequencing (sRNA-seq), miRNA microarrays and real-time quantitative PCR (RT-qPCR) assays are currently used to detect and quantify miRNAs, and each approach has strengths and weaknesses.[20–23] The strengths of sRNA-seq include unbiased characterization of the miRNA transcriptome at a genome-wide level, resolution at the single nucleotide level, low background noise and measurement of transcript abundance over a broad dynamic range. It is the preferred approach for the discovery phase but requires considerable technical skills and bioinformatics support. sRNA-seq is also less sensitive in detecting and quantifying miRNAs compared to RT-qPCR assays. miRNA microarrays are customized to detect a prespecified set of miRNAs whose sequences must be known a priori and is semi quantitative. miRNA-specific RT-qPCR assays have high sensitivity and specificity, but the conventional cycle threshold (Ct) method used to compute transcript abundance yields relative rather than absolute miRNA copy number.

In the current study, we used a stepwise approach that leveraged the strengths and minimized weaknesses associated with each miRNA profiling platform. We used sRNA-seq to discover circulating miRNAs associated with liver allograft biopsy diagnosis. sRNA-seq was refined by incorporating synthetic RNAs to monitor RNA recovery from sera and to monitor cDNA library-preparation. We used human TaqMan low-density arrays (TLDA) to confirm the miRNAs prioritized by sRNA-seq and bioinformatics. The preamplification step, integral to the human TaqMan® Array protocol, ensured sufficient cDNA for absolute quantification of miRNA copy number using the customized RT-qPCR assays developed in our laboratory.[14] Our use of an in-house developed Bak amplicon eliminated limitations inherent to the comparative Ct method for miRNA quantification and enabled measurement of absolute copy numbers of miRNAs.

We first profiled sera matched to liver allograft biopsies classified as no rejection (NR) biopsies and sera matched to acute rejection (AR) biopsies. To avoid confounding of AR biopsy diagnosis by intragraft inflammation due to recurrent hepatitis C virus (R-HCV) or other autoimmune hepatitis, we developed AR prediction models using sera from patients who needed liver transplantation due to nonimmune, nonviral (NINV) liver disease, and excluded sera from patients who needed liver transplantation due to HCV, other viral or autoimmune hepatitis. Following identification of miRNAs associated with AR in the pristine NINV cohort, we prioritized these miRNAs for analysis of sera from liver allograft recipients with R-HCV and examined whether the miRNAs associated with AR in the NINV cohort are also diagnostic of intragraft inflammation or fibrosis due to R-HCV. Herein, we report miRNAs and candidate prediction models for accurate diagnosis of AR in human liver allografts, and the ability of the AR-associated miRNAs to discriminate intragraft inflammation due to AR from intragraft inflammation or fibrosis due to R-HCV.

MATERIALS AND METHODS

Biospecimens and Study Cohorts

Sera from adult recipients of deceased donor liver allografts (patients) enrolled in the “Immune Tolerance Network Immunosuppression withdrawal study” (ITN030ST, ClinicalTrials.gov identifier: NCT00135694) were profiled in the Clinical Trials of Transplantation (CTOT)-07 study (NCT01428700) to determine whether circulating levels

of extracellular miRNAs are diagnostic of AR or R-HCV in human liver allograft recipients. The Inclusion and Exclusion Criteria for the CTOT-07 study are provided as Supplemental Digital Content (SDC).

Table S1A shows the demographics of the 26 unique NINV patients and Table S1B shows the demographics of the 41 unique R-HCV patients profiled in this study. All biopsies were analyzed by the parent study pathologist and classified using the Banff schema and biopsy codes (Table S1C) for grading biopsy features[24] and were made prior to miRNA profiling of sera matched to biopsies. The biopsies from the NINV cohort were classified as acute rejection (AR) or no rejection (NR). The biopsies from the R-HCV cohort were classified as biopsies without intragraft inflammation or fibrosis (R-HCV-N), biopsies with inflammation (R-HCV-I) or biopsies with fibrosis (R-HCV-F). A total of 91 sera matched to 91 liver allograft biopsies, 30 sera matched to 30 biopsies from the NINV cohort and n=61 sera matched to 61 biopsies from the R-HCV cohort were profiled for circulating levels of miRNAs. Additional details are provided as SDC.

All patients provided written informed consent for participation in the study. The Institutional Review Boards at Weill Cornell Medicine and Rockefeller University approved miRNA profiling of sera.

Small RNA Sequencing: NINV cohort

Figure 1 illustrates our study design. We determined global miRNA abundance in circulation by sRNA-seq, as developed in the Tuschl laboratory.[13,25] The samples were spiked with 2 cocktails of synthetic RNAs, the first cocktail (Table S2A) to monitor RNA recovery and the second cocktail (Table S2B) to monitor cDNA library preparation.[13,26] The FASTQ output files were analyzed, as described.[13,26] Three sera matched to NR biopsies, and 1 serum matched to an AR biopsy were excluded from downstream analysis because of the skewed distribution of spiked-in synthetic RNAs (Table S3 and Figure S1). Additional details are provided as SDC.

Differential Gene Abundance Analysis

Exact test of the R/Bioconductor package edgeR (version 3.8.2)[27] was used to assess differences in miRNA abundance between AR sera and NR sera and R statistical language (version 3.1.2) was used for data analysis. Heatmaps and unsupervised clustering were created with the ‘aheatmap’ function of the NMF R package (version 0.20.5)[28] using Euclidean distance and complete-linkage clustering for rows (miRNAs) and columns (samples). Additional details are provided as SDC.

Microarray Profiling: NINV Cohort

We used pristine aliquots of 100μl of serum to isolate RNA for the measurement of miRNAs using TLDA Human MicroRNA A Card v2.0 containing primers and probes for the amplification of 377 miRNA targets and 4 control assays (Life Technologies catalog number 4398965). The serum sample was spiked with 5μl of 1nM synthetic cel-miR-54 (5’-UACCCGUAAUCUUCAUAAUCCGAG-3’, Integrated DNA Technologies) as a quality control measure. We isolated RNA using Qiagen miRNeasy mini kit (cat no. 217004).

We used the Applied Biosystems' 7900HT Fast Real-Time PCR System to run the RT-PCR reactions and used DataAssist™ Software v3.01 (Life Technologies) to calculate the relative abundance of miRNAs, fold change, and the Benjamini-Hochberg false discovery rate-adjusted *P*-values. We excluded any Ct value > 35 from data analysis. Additional details are provided as SDC.

Customized RT-qPCR assays: NINV cohort and R-HCV cohort

Absolute copy numbers of the serum miRNAs identified by both sRNA-seq and TLDA as being significantly associated with AR in the NINV cohort were quantified using customized RT-qPCR assays (Figure 1). Absolute levels of miRNAs included in the 2 best NINV-AR models were quantified in sera from the R-HCV cohort using customized RT-qPCR assays. Additional details are provided as SDC.

Statistical Analysis

Mann-Whitney test and Fisher's exact test were used for group comparisons of continuous variables and categorical variables, respectively. Logistic regression analyses for discriminating biopsies classified as NINV-NR, NINV-AR, R-HCV-N, R-HCV-I or R-HCV-F were performed using the $\log_e$–transformed ratios of miRNA copy number to cel-miR-54 copy number ($x10^{-8}$) as predictors. Area under the receiver operating characteristic (AUROC) curve was calculated as a measure of discrimination. Logistic regression was used to generate diagnostic signatures based on combinations of miRNAs for which the resulting AUROC was again calculated. The cut point that yielded the highest combined sensitivity and specificity (Youden's index) for predicting biopsy diagnosis was determined. The Akaike information criterion (AIC) and Akaike weight (AW) were used to compare regression models. Bootstrap resampling was performed to estimate robust 95% confidence intervals (95% CI) of the AUROC for the best models.[29] All analyses were performed using SAS 9.4 (SAS Institute, Cary, NC).

RESULTS

Patients and Liver Allograft Biopsies: NINV cohort

The characteristics of the NINV cohort are summarized in Table 1; additional details, including histological features of each biopsy, are provided in Table S1A. The time from transplantation to biopsy, the type of biopsy (for-cause vs. protocol), and liver function tests differed between the AR group and the NR group.

Serum Transcriptomics

We obtained on average of 4 million miRNA reads per serum sample (range 83,000–38 million) by sRNA-seq representing 11–68% of all reads in the 13 sera matched to 13 AR biopsies (AR sera) from 12 patients and 13 sera matched to 13 no rejection biopsies (NR sera) from 12 patients. Unlike previous reports,[13,25,30] very few reads in this study were annotated as transfer RNA fragments due to 19–24 nt size selection in this study during the sRNA-seq library preparation.

The most abundant miRNAs were those present at high copy numbers in hematopoietic cells, endothelial cells and hepatocytes (Figure 2A and B).[13,31] Unsupervised hierarchical clustering showed that 22 of the 26 sera were successfully grouped by biopsy diagnosis (Figure 2A). Composition analysis showed that the relative frequencies of 25 miRNAs differed (false discovery rate-adjusted *P* [FDR-*P*] ≤0.15) between AR sera and NR sera (Table 2). The liver-specific miR-122 was 7.9-fold higher (FDR-*P*=0.0001). The cistronic and therefore co-transcribed miR-192 and −194 are also characteristic for liver tissue, although not as specifically or as abundantly expressed as miR-122 (Figure 2B).[31] The magnitude of the observed differences ranged from 27-fold lower to 14-fold higher. The increase of liver-typic miRNAs in AR sera was positively associated with the circulating levels of ALT and AST (Figure 2A and C).

Among the 18 miRNAs identified by sRNA-seq to be more frequent in AR sera vs. NR sera at FDR-P≤0.15, the relative abundance of 9 miRNAs – miR-22, miR-34a, miR-122, miR-148a, miR-192, miR-193b, miR-194, miR-210 and miR-885–5p – were also higher in AR sera vs. NR sera at the same FDR-*P*≤0.15 when the sera were profiled using TLDA. We prioritized these 9 miRNAs for absolute quantification using customized RT-qPCR assays developed in our laboratory.

Absolute Quantification of miRNAs

Absolute quantification of miRNA copy numbers using customized RT-qPCR assays confirmed the higher abundance of all 9 miRNAs in AR sera vs. NR sera (Table S4). Figure 3 shows violin plots portraying the distribution of $\log_e$ transformed ratios of miRNA copy number to cel-miR-54 copy number ($x10^{-8}$) in the 14 AR sera and the 16 NR sera (Figure 3A–I). The higher abundance in AR sera vs. NR sera was miRNA specific since the level of endogenous U6 snRNA was not different between the 2 groups (Figure 3K, *P*=0.80; Figure 3L, *P*=0.43, Mann-Whitney test). Nonspecific factors for the differential levels in AR sera and NR sera can also be excluded because the spiked-in control cel-miR-54 level was not different between the 2 groups (Figure 3J, *P*=0.43).

Logistic Regression Analysis

Univariate logistic regression analysis predicting AR vs.NR was performed with $\log_e$ ratios of miRNA copy number to cel-miR-54 copy number ($x10^{-8}$) as predictors. The likelihood-ratio chi-square statistic and associated *P* value, goodness-of-fit using AIC and AW, and AUROC along with 95% CI for each of the 9 predictors are shown in Table S5.

Development of Diagnostic Models

From all-2-miRNA logistic regression models, we identified the best statistical model for discriminating AR group from NR group. The logistic model of −291.3 + (40.66*miR-210) + (12.88*miR-34a) yielded an AUROC of 1.0, and the cut point of −0.35 (Youden's index) classified all 30 sera with 100% accuracy (Likelihood Ratio $\chi 2$= 40.09, *P*=2.42E-10). A comparison of AUROCs of all 36 possible combinations of 2 miRNAs showed that the AUROC of miR-210 + miR-34a was not significantly larger than the AUROCs of any of the other 35 possible combinations or even the AUROCs of any single miRNA except that of miR-148 (Table S5). However, evaluation of goodness-of-fit using AIC showed that the

miR-210 + miR-34a combination is superior to all other 2- miRNA prediction models (Table S5). Furthermore, the AW for miR-210 + miR-34a model was 84% (Table S5).

Because miR-122 is a liver specific miRNA, we systematically examined the diagnostic performance of all combinations of miR-122 with 1 of the other 8 miRNAs. A linear combination of miR-122 + miR-210 yielded the largest AUROC (0.99, 95% CI, 0.97 to 1.00, $P<0.0001$) compared to all other combinations (Table 3). Although the AUROCs were not different among the 8 combinations, evaluation of the goodness-of-fit using AIC showed that the miR-122 + miR-210 combination was superior to all other 2-miRNA prediction models with the possible exemption of miR-122 + miR-194 (Table S5).

Bootstrap analysis with 10,000 replications yielded bias-corrected 95% CI for the AUROC of 1.0–1.0 for the best-fit statistical model of miR-210 + miR-34a model and 0.929–1.000 for the best fitting model that included miR-122 (Table 4).

Figure 4 displays the predicted probability of AR based on the best-fit statistical model of miR-210 + miR-34a (Panel A) or the linear combination of miR-122 plus each of the 8 miRNAs (Panels B-I). The miR-210 + miR-34a model classified all 30 sera perfectly and the miR-122 + miR-210 model classified 29 of 30 sera correctly.

Time from transplantation to biopsy differed between NINV-AR vs. NINV-NR (Table 1). Circulating levels of miRNAs were diagnostic of NINV-AR after controlling for time since transplantation to biopsy (Table S6)

R-HCV Cohort

The characteristics of the R-HCV cohort, stratified by liver allograft biopsy diagnosis, are summarized in Table 5. Additional information, including histological features of each biopsy, is provided in Table S1B. miR-34a, miR-122 and miR-210, the miRNAs diagnostic of AR in the NINV cohort and included in our AR diagnostic models, were prioritized for quantification using customized RT-qPCR assays and data analyzed to address: (i) Do serum miRNA levels discriminate patients with R-HCV-N, R-HCV-I, or R-HCV-F biopsies? (ii) Do serum miRNA levels discriminate NINV patients with NR biopsies from those with R-HCV-N, R-HCV-I or R-HCV-F biopsies? (iii) Do serum miRNAs levels discriminate NINV patients with AR biopsies from those with R-HCV-N, R-HCV-I or R- HCV-F biopsies?

Levels of miR-34a, miR-122 and miR-210 were measured in 19 sera matched to 19 R-HCV-N biopsies, 27 sera matched to 27 R-HCV-I biopsies, and 15 sera matched to 15 R-HCV-F biopsies. Table S7 shows the Ct values (Table S7A), absolute copy numbers (Table S7B) and $\log_e$ ratios of serum miRNA copies to cel-miR-54 copies ($x10^{-8}$) (Table S7C) in sera matched to biopsies.

Table 6 shows the log-likelihood *P* values from logistic regressions assessing the ability of serum miRNA levels to discriminate each combination of 2 biopsy groups. Circulating levels of miR-34a and miR-122 were higher in R-HCV-I group compared to R-HCV-N group, and miR-34a level was higher in R-HCV-F group vs. R-HCV-N group. None of the 3 miRNAs differentiated the HCV-I group from the HCV-F group.

Levels of miR-34a and miR-122 but not miR-210 level were higher in R-HCV-N group vs. NINV-NR group and all 3 miRNAs were higher in the R-HCV-I group and the R-HCV-F group compared to the NINIV-NR group. A comparison of levels in the NINV-AR group with the R-HCV-I or the R-HCV-F group showed miRNA-specific alterations: miR-34a level was higher and miR-210 lower in both R-HCV-I and R-HCV-F groups compared to the NINV-AR group and miR-122 levels were not different between the NINV-AR group and either R-HCV-I group or R-HCV-F group (Table 6). Because of the differential directionality of miR-34a and miR-210 levels, we performed additional logistic regression analyses to identify the best prediction models to discriminate NINV-AR group from R-HCV-I group and NINV-AR group from R-HCV-F group.

ROC curve analyses portraying the extent to which circulating levels of miRNA distinguish NINV-AR group from R-HCV-I group and NINV-AR group from R-HCV-F group are shown in Figure 5. miR-34a (P <0.0001, 5A); miR-210 (P=0.02, 5C); miR-34a + miR-210 (P<0.0001, 5D); and miR-34a + miR-122 (P<0.0001, 5E) discriminated NINV-AR group from R-HCV-I group. miR-34a (P <0.0001, 5F); miR-210 (P=0.02, 5H); miR-34a + miR-210 (P<0.0001, 5I); and miR-34a + miR-122 (P<0.0001, 5J) discriminated NINV AR from R-HCV-F group.

Table 7 shows the AUROCs (95% CI), diagnostic signature cut point, sensitivity, specificity and accuracy for miR-34a, miR-122, miR-210 and for the 2 2-miR models along with their logistic regression equations for discriminating NINV-AR group from R-HCV-I group (Table 7A) and NINV-AR group from R-HCV-F group (Table 7B). We identified that a combination of miR-34a + miR-210 and a combination of miR-34a +miR-122 discriminate NINV-AR group from R-HCV-I group with AUROCs of 1.00 (1.00–1.00, P<0.0001 for both models) (Table 7A) and that these 2 models discriminate NINV-AR group from R-HCV-F group with an AUROC of 0.99 (0.97–1.00, P<0.0001) and an AUROC of 1.0 (1.00–1.00, P<0.0001), respectively (Table 7B). AIC and Akaike weight related to these analyses are provided in Table S8.

Among the liver function tests, alkaline phosphatase (ALP) level discriminated NINV-AR from R-HCV-I (P=0.027) and R-HCV-F (P=0.02) (Table S9A). In the analysis restricted to for-cause biopsies, ALP did not discriminate NINV-AR from R-HCV-I (P=0.25) but miR-34a level (P=0.0016) and the prediction model miR-34a + mIR-210 discriminated NINV-AR from R-HCV-I (P<0.0001) (Table S9B). Neither liver function tests nor miRNAs discriminated R-HCV-I group from R-HCV-F group (Table S10).

DISCUSSION

Using sRNA-seq and miRNA microarrays to profile biopsy matched sera from the NINV cohorts, we identified 9 miRNAs diagnostic of AR in human liver allografts. We measured absolute levels of these 9 miRNAs using customized RT-qPCR assays, and using logistic regression found that a combination of miR-34a and miR-210 is the best statistical predictor of AR in the NINV cohort. Since a prediction model that includes miR-122 may authenticate hepatocyte injury, we evaluated models that included miR-122, and identified that a combination of miR-122 + miR-210 is the best of 8 models that included miR-122.

Following authentication that miR-34a, miR-122 and miR-210 distinguish between liver allografts with or without intragraft inflammation under pristine settings not confounded by R-HCV, we examined whether these 3 miRNAs also discriminate NINV-AR group from R-HCV-I or R-HCV-F group.

Circulating level of miR-34a was substantially higher in R-HCV-I and R-HCV-F groups compared to NINV-AR group. HCV stimulates nuclear factor kappa B (NF-κB) expression[32] and NF-κB is a transcriptional activator of miR-34a.[33] The NF-κB pathway might be responsible for the high miR-34a levels in the R-HCV group. HCV native liver disease has also been associated with high level of miR-34a.[34]

We confirm and extend earlier reports[18,35,36] that circulating levels of miR-122 are higher in the NINV-AR group than in the NINV-NR group. Whereas miRNAs are known for translational repression, miR-122 uniquely stimulates HCV replication[37] and the increased HCV replication and associated hepatocyte injury may contribute to the high circulating levels of miR-122 level in the R-HCV group. A novel observation from our study is the decreased abundance of 3' end adenylated miR-122 molecules in NINV-AR sera compared to NINV- NR sera (Figure S2). 3' end adenylation is reported to impact miR-122 stability and its function[38] and whether this is an additional mechanism for the high levels of miR-122 in R-HCV cohort is not known.

miR-210 has been associated with hypoxia and hepatic cell injury and inflammation.[39,40] Hypoxia and hepatic inflammation associated with NINV-AR, R-HCV-I or R-HCV-F may have contributed to the higher abundance of miR-210 in these groups compared to the NINV-NR group.

Serum levels of miR-34a, miR-122 and miR-210 were all higher in NINV-AR vs. NINV-NR and linear combinations of miR-34a + miR-210 and miR-122 + miR-210 distinguished these 2 groups very accurately. The logistic regression equations for the models developed to distinguish NINV-AR from NINV-NR wherein both miR-34a and miR-210 were higher in NINV-AR vs. NINV NR were not optimal for discriminating NINV-AR from R-HCV-I or R-HCV-F group since miR-34a level was lower and level of miR-210 was higher in the NINV-AR group compared to R-HCV-I and R-HCV-F groups. The logistic regression equations incorporating the differential abundance of miR-34a and miR-210 discriminated NINV-AR from R-HCV-I or R-HCV-F with near perfection.

Although miR-34a, miR-122 or miR-210 discriminated R-HCV-N from R-HCV-I or R-HCV-F group, none differentiated R-HCV-I from R-HCV-F group. This is not surprising since the inflammation grade was similar in R-HCV-I biopsies and R-HCV-F biopsies and these miRNAs were selected on the basis of their ability to identify intragraft inflammation in NINV-AR biopsies. Like miRNAs profiled here, none of the liver function tests discriminated the R-HCV-I from R-HCV-F group. In this regard, it has been reported that serum levels of miR-19a and miR-20a discriminate R-HCV classified as slow fibrosis progressors from fast fibrosis progressors.[41]

The signatures we developed to discriminate AR from R-HCV-I or R-HCV-F have not been investigated to determine whether these prediction models distinguish additional causes of

intragraft inflammation and fibrosis. This critical question should be addressable by deep profiling of additional cohorts.

Our study suggests that quantification of miRNAs in serum using RT-qPCR assays is sufficient for accurate diagnosis of NINV-AR, R-HCV-I or R-HCV-F in human liver allografts. RT-qPCR assays are widely used to manage allograft recipients (eg, to measure CMV abundance in blood) and the turnaround time of 4 to 6 hours is useful for clinical decision making. RT-qPCR assay is also economical with an estimated $150 cost for measuring 3–5 miRNAs compared to sRNA-seq or microarray profiling. RT-qPCR assay-based measurements represent a practical approach to monitor liver allograft recipients.

Our study has limitations. The sample size is relatively small, and our models were not validated using external cohorts and may be overfit. sRNA-seq and miRNA microarray profiling of biopsy-matched sera informed prioritization of miRNAs for quantification in sera matched to NINV-AR and NINV-NR biopsies whereas the abundance of miR-34a, miR-122 and miR-210 in sera from R-HCV-N, RCV-I and RCV-F groups were prioritized for data analyses based on NINV-AR prediction models. Additional candidate miRNA models could emerge by scRNA-Seq of sera from the R-HCV cohorts. We also did not investigate whether an increase in miRNA levels precedes an increase in transaminase levels or predicts future intragraft pathology. Existing data suggest that miRNAs are more sensitive than liver enzymes in detecting liver injury and also help anticipate acute rejection.[18,41] Indeed, circulating levels of miRNAs outperformed liver enzymes in our study, and in an analysis restricted to for-cause biopsies, miRNAs discriminated NINV-AR group from R-HCV-I group whereas the liver enzymes did not.

Sera from patients enrolled in the parent “Immune Tolerance Network Immunosuppression withdrawal study” were profiled in our investigation. The study participants underwent both for-cause biopsies and protocol-specified biopsies. Whether the miRNA profiles identified in systematized trials are generalizable to routine clinical settings remain to be determined.

In sum, we performed sRNA-seq to discover miRNAs diagnostic of AR, miRNA microarrays to verify the discovered biomarkers and customized RT-qPCR assays for absolute quantification of miRNAs. Our stepwise approach identified candidate models containing miR-34a, miR-122 and miR-210 that discriminated NINV-AR group from NINV-NR group very accurately. The miRNAs were diagnostic of even borderline/mild AR in human liver allografts. These 3 miRNAs discriminated also NINV-AR group from R-HCV-I or R-HCV-F group with high precision. Noninvasive detection of intragraft pathology at an early stage may be of great value for personalizing immunosuppression and for monitoring patients treated with direct acting anti-HCV therapy.

Supplementary Material

Refer to Web version on PubMed Central for supplementary material.

ACKNOWLEDGMENTS

We thank Dr. Nancy Bridges (NIAID, NIH) and Ms. Tina Sledge (NIAID, NIH) for their invaluable help in obtaining the precious serum samples from the liver allograft recipients enrolled in the “Immune Tolerance Network Immunosuppression withdrawal study (ITN030ST, ClinicalTrials.gov identifier: NCT00135694). We are deeply appreciative of Dr. Abraham Shaked, the Principal Investigator of the parent trial ITN030ST for the study design that included collection of serum samples matched to liver allograft biopsies from recipients with nonimmune nonviral cause for native liver disease or HCV as the cause for liver disease. The liver allograft biopsy-matched serum samples were provided to Manikkam Suthanthiran, MD at Cornell University to perform serum miRNA profiling proposed in “Development of Gene Expression Signatures for the Diagnosis of Liver Allograft Rejection and Recurrent Hepatitis C Disease” (Clinical Trials in Transplantation-07; ClinicalTrials.gov identifier: NCT01428700; Principal Investigator: Abraham Shaked, MD, PhD, University of Pennsylvania School of Medicine; Protocol Chair: Manikkam Suthanthiran, MD, Cornell University).

Funding

Supported in part by awards from the National Institutes of Health (UO1AI63589, R37AI051652, and NIH UH2/UH3 TR000933). T.M. is the recipient of awards (K08-DK087824 and R03-DK105270) from the NIDDK, NIH. H.B. was partly supported by the National Center for Advancing Translational Sciences, National Institutes of Health, through grant UL1 TR 000002.

T.T. is a cofounder of and scientific advisor to Alnylam Pharmaceuticals and a scientific advisor to Regulus Therapeutics. M.S. has a Consultancy Agreement with CareDx, Inc. Brisbane, CA and with Sparks Therapeutics, Philadelphia, PA.

ABBREVIATIONS

ALT	alanine aminotransferase
AP	alkaline phosphatase
AST	aspartate aminotransferase
AUROC	area under the receiver operating characteristic curve
cDNA	complementary DNA
CTOT-07	Clinical Trials of Transplantation-07
FDR-P	false discovery rate-adjusted P value
HCV	hepatitis C virus
mRNA	messenger RNA
miRNA	micro RNA
RT-qPCR	real-time quantitative polymerase chain reaction
sRNA-seq	small RNA sequencing
TLDA	TaqMan® low density arrays

REFERENCES

1. Kwong A, Kim WR, Lake JR, et al. OPTN/SRTR 2018 annual data report: liver. Am J Transplant. 2020;20 Suppl s1:193–299. [PubMed: 31898413]
2. Adams DH, Sanchez-Fueyo A, Samuel D. From immunosuppression to tolerance. J Hepatol. 2015;62(Suppl 1):S170–S185. [PubMed: 25920086]

3. Cillo U, Bechstein WO, Berlakovich G, et al. Identifying risk profiles in liver transplant candidates and implications for induction immunosuppression. Transplant Rev (Orlando). 2018;32(3):142–150. [PubMed: 29709248]
4. Levitsky J. Operational tolerance: past lessons and future prospects. Liver Transpl. 2011;17(3):222–232. [PubMed: 21384504]
5. Demetris AJ, Bellamy C, Hübscher SG, et al. 2016 comprehensive update of the Banff Working Group on liver allograft pathology: introduction of antibody-mediated rejection. Am J Transplant. 2016;16(10):2816–2835. [PubMed: 27273869]
6. Bubak ME, Porayko MK, Krom RA, et al. Complications of liver biopsy in liver transplant patients: increased sepsis associated with choledochojejunostomy. Hepatology. 1991;14(6):1063–1065. [PubMed: 1959854]
7. Rockey DC, Caldwell SH, Goodman ZD, et al. ; American Association for the Study of Liver Diseases. Liver biopsy. Hepatology. 2009;49(3):1017–1044. [PubMed: 19243014]
8. Van Thiel DH, Gavaler JS, Wright H, et al. Liver biopsy. Its safety and complications as seen at a liver transplant center. Transplantation. 1993;55(5):1087–1090. [PubMed: 8497887]
9. Shaked A, DesMarais MR, Kopetskie H, et al. Outcomes of immunosuppression minimization and withdrawal early after liver transplantation. Am J Transplant. 2019;19(5):1397–1409. [PubMed: 30506630]
10. Bartel DP. MicroRNAs: genomics, biogenesis, mechanism, and function. Cell. 2004;116(2):281–297. [PubMed: 14744438]
11. Kaul V, Krams S. MicroRNAs as master regulators of immune responses in transplant recipients. Curr Opin Organ Transplant. 2015;20(1):29–36. [PubMed: 25563989]
12. Mehta A, Baltimore D. MicroRNAs as regulatory elements in immune system logic. Nat Rev Immunol. 2016;16(5):279–294. [PubMed: 27121651]
13. Akat KM, Moore-McGriff D, Morozov P, et al. Comparative RNA-sequencing analysis of myocardial and circulating small RNAs in human heart failure and their utility as biomarkers. Proc Natl Acad Sci U S A. 2014;111(30):11151–11156. [PubMed: 25012294]
14. Anglicheau D, Sharma VK, Ding R, et al. MicroRNA expression profiles predictive of human renal allograft status. Proc Natl Acad Sci U S A. 2009;106(13):5330–5335. [PubMed: 19289845]
15. Das S, Ansel KM, Bitzer M, et al. ; Extracellular RNA Communication Consortium. The Extracellular RNA Communication Consortium: establishing foundational knowledge and technologies for extracellular RNA research. Cell. 2019;177(2):231–242. [PubMed: 30951667]
16. Khan Z, Suthanthiran M, Muthukumar T. MicroRNAs and transplantation. Clin Lab Med. 2019;39(1):125–143. [PubMed: 30709501]
17. Mitchell PS, Parkin RK, Kroh EM, et al. Circulating microRNAs as stable blood-based markers for cancer detection. Proc Natl Acad Sci U S A. 2008;105(30):10513–10518. [PubMed: 18663219]
18. Shaked A, Chang BL, Barnes MR, et al. An ectopically expressed serum miRNA signature is prognostic, diagnostic, and biologically related to liver allograft rejection. Hepatology. 2017;65(1):269–280. [PubMed: 27533743]
19. Ward J, Kanchagar C, Veksler-Lublinsky I, et al. Circulating microRNA profiles in human patients with acetaminophen hepatotoxicity or ischemic hepatitis. Proc Natl Acad Sci U S A. 2014;111(33):12169–12174. [PubMed: 25092309]
20. Git A, Dvinge H, Salmon-Divon M, et al. Systematic comparison of microarray profiling, real-time PCR, and next-generation sequencing technologies for measuring differential microRNA expression. RNA. 2010;16(5):991–1006. [PubMed: 20360395]
21. Hardikar AA, Farr RJ, Joglekar MV. Circulating microRNAs: understanding the limits for quantitative measurement by real-time PCR. J Am Heart Assoc. 2014;3(1):e000792.
22. Mestdagh P, Hartmann N, Baeriswyl L, et al. Evaluation of quantitative miRNA expression platforms in the microRNA quality control (miRQC) study. Nat Methods. 2014;11(8):809–815. [PubMed: 24973947]
23. Redshaw N, Wilkes T, Whale A, et al. A comparison of miRNA isolation and RT-qPCR technologies and their effects on quantification accuracy and repeatability. Biotechniques. 2013;54(3):155–164. [PubMed: 23477383]

24. Banff Working Group on Liver Allograft Pathology. Importance of liver biopsy findings in immunosuppression management: biopsy monitoring and working criteria for patients with operational tolerance. Liver Transpl. 2012;18(10):1154–1170. [PubMed: 22645090]
25. Hafner M, Renwick N, Farazi TA, et al. Barcoded cDNA library preparation for small RNA profiling by next-generation sequencing. Methods. 2012;58(2):164–170. [PubMed: 22885844]
26. Farazi TA, Horlings HM, Ten Hoeve JJ, et al. MicroRNA sequence and expression analysis in breast tumors by deep sequencing. Cancer Res. 2011;71(13):4443–4453. [PubMed: 21586611]
27. Robinson MD, McCarthy DJ, Smyth GK. edgeR: a Bioconductor package for differential expression analysis of digital gene expression data. Bioinformatics. 2010;26(1):139–140. [PubMed: 19910308]
28. Gaujoux R, Seoighe C. A flexible R package for nonnegative matrix factorization. BMC Bioinformatics. 2010;11:367. [PubMed: 20598126]
29. Davison A, Hinkley D. Bootstrap Methods and their Application (Cambridge Series in Statistical and Probabilistic Mathematics). Cambridge University Press; 1997.
30. Dhahbi JM, Spindler SR, Atamna H, et al. 5' tRNA halves are present as abundant complexes in serum, concentrated in blood cells, and modulated by aging and calorie restriction. BMC Genomics. 2013;14:298. [PubMed: 23638709]
31. Landgraf P, Rusu M, Sheridan R, et al. A mammalian microRNA expression atlas based on small RNA library sequencing. Cell. 2007;129(7):1401–1414. [PubMed: 17604727]
32. Tai DI, Tsai SL, Chen YM, et al. Activation of nuclear factor kappaB in hepatitis C virus infection: implications for pathogenesis and hepatocarcinogenesis. Hepatology. 2000;31(3):656–664. [PubMed: 10706556]
33. Li J, Wang K, Chen X, et al. Transcriptional activation of microRNA-34a by NF-kappa B in human esophageal cancer cells. BMC Mol Biol. 2012;13:4. [PubMed: 22292433]
34. Cermelli S, Ruggieri A, Marrero JA, et al. Circulating microRNAs in patients with chronic hepatitis C and non-alcoholic fatty liver disease. PLoS One. 2011;6(8):e23937.
35. Farid WRR, Pan Q, van der Meer AJP, et al. Hepatocyte-derived microRNAs as serum biomarkers of hepatic injury and rejection after liver transplantation. Liver Transpl. 2012;18(3):290–297. [PubMed: 21932376]
36. Ruiz P, Millán O, Ríos J, et al. MicroRNAs 155–5p, 122–5p, and 181a-5p identify patients with graft dysfunction due to T cell-mediated rejection after liver transplantation. Liver Transpl. 2020;26(10):1275–1286. [PubMed: 32615025]
37. Jopling CL. Regulation of hepatitis C virus by microRNA-122. Biochem Soc Trans. 2008;36(Pt 6):1220–1223. [PubMed: 19021529]
38. Sanei M, Chen X. Mechanisms of microRNA turnover. Curr Opin Plant Biol. 2015;27:199–206. [PubMed: 26342825]
39. Krauskopf J, Caiment F, Claessen SM, et al. Application of high-throughput sequencing to circulating microRNAs reveals novel biomarkers for drug-induced liver injury. Toxicol Sci. 2015;143(2):268–276. [PubMed: 25359176]
40. Song G, Jia H, Xu H, et al. Studying the association of microRNA-210 level with chronic hepatitis B progression. J Viral Hepat. 2014;21(4):272–280. [PubMed: 24597695]
41. Joshi D, Salehi S, Brereton H, et al. Distinct microRNA profiles are associated with the severity of hepatitis C virus recurrence and acute cellular rejection after liver transplantation. Liver Transpl. 2013;19(4):383–394. [PubMed: 23408392]

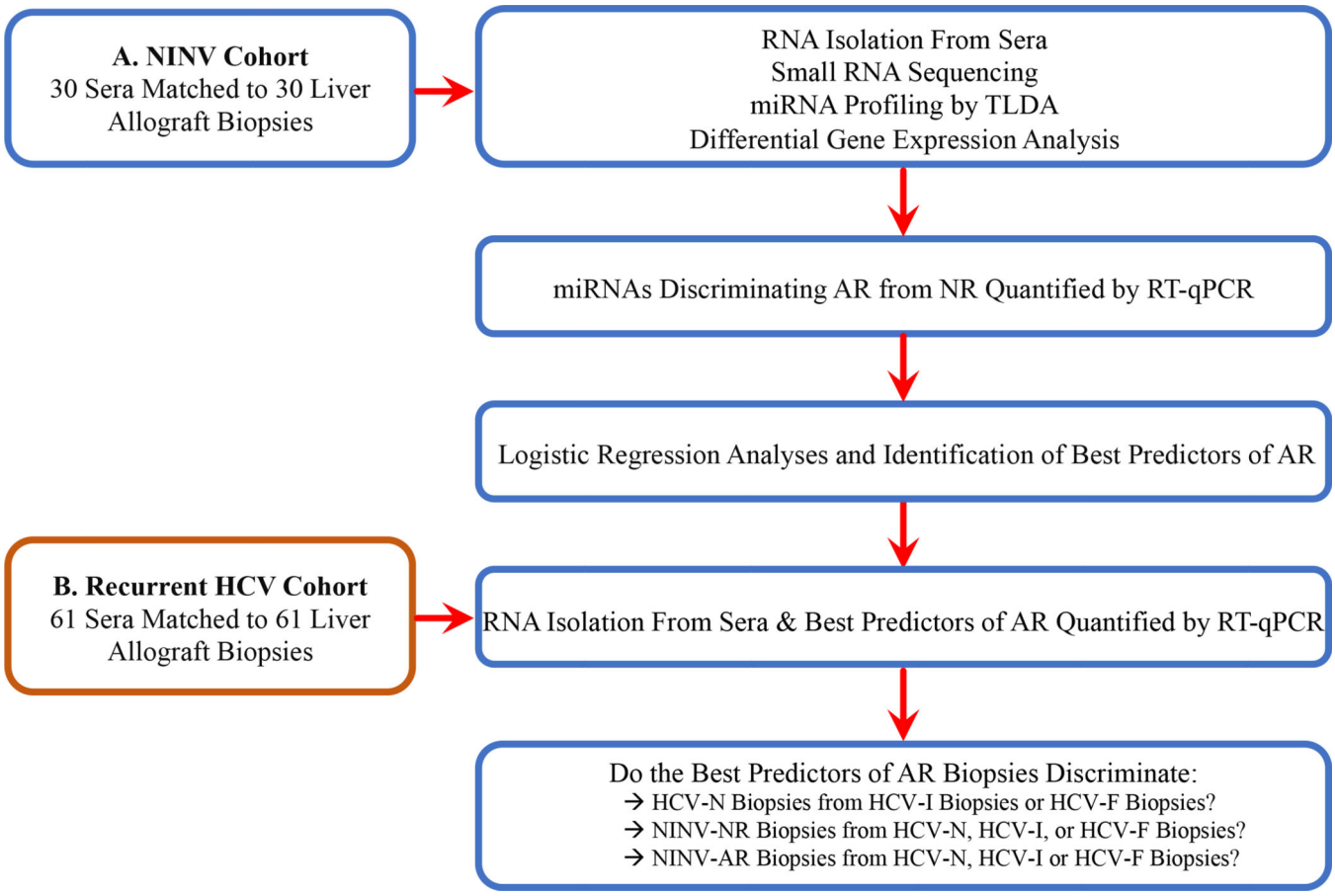

Figure 1. Flowchart illustrating the sequential steps used to identify circulating extracellular miRNAs diagnostic of human liver allograft biopsies.

A, NINV Cohort: Total RNA was isolated from 30 sera matched to 30 allograft biopsies from 26 unique liver allograft recipients with nonimmune nonviral (NINV) etiology for their native liver disease. Among the 30 sera, 14 were matched to 14 acute rejection (AR) biopsies from 12 recipients (2 patients had 2 AR biopsies) and 16 were matched to 16 no rejection (NR) biopsies from 14 recipients (1 patient had 2 NR biopsies and 1 patient with an initial AR biopsy had a later NR biopsy and is included in both groups). Table 1 and Table S1A provide additional information regarding the NINV cohort including liver allograft biopsy findings for each biopsy. Barcoded complementary DNA libraries were prepared from the RNA isolated from the biopsy-matched sera and small RNA sequenced for unbiased characterization of the circulating micro RNA (miRNA) transcriptomes. A TaqMan low-density array (TLDA) was used to measure relative levels of 377 mature human miRNAs in sera matched to biopsies. Differential gene abundance analysis was performed to identify miRNAs that discriminate the AR biopsy group from the NR biopsy group. Absolute levels of miRNAs discriminating AR group from NR group were quantified using customized real time quantitative polymerase chain reaction (RT-qPCR) assays. Area under the receiver operating characteristic curve was calculated as a measure of discrimination. Logistic regression analyses were performed and goodness-of-fit using Akaike's information criterion and Akaike weight were used to evaluate candidate models for discriminating

AR group from NR group. Bootstrap analysis was performed for the best-fit models.

B, Recurrent Hepatitis C Virus (HCV) Cohort: Total RNA was isolated from 61 sera matched to 61 allograft biopsies from 41 unique liver allograft recipients with HCV native liver disease. Among the 61 sera, 19 were matched to 19 liver allograft biopsies without intragraft inflammation or fibrosis and classified as normal biopsies (recurrent HCV-N); 27 were matched to liver allograft biopsies with intragraft inflammation (recurrent HCV-I); and 15 were matched to 15 liver allograft biopsies with intragraft fibrosis (recurrent HCV-F). Table 6 and Table S1B provide additional information regarding the recurrent HCV cohort including liver allograft biopsy findings for each biopsy. Table 6 also provides information regarding recurrent HCV patients who underwent multiple biopsies with different biopsy classification (eg, HCV-N on initial biopsy and HCV-I in a later biopsy). Total RNA was isolated from each serum sample and absolute levels of miR-34a, miR-122 and miR-210- the components of the 2 diagnostic signatures for discriminating AR biopsies from NR biopsies in the NINV cohort- were quantified using customized RT-qPCR assays. Logistic regression analyses were performed to address the following: (i) Do the best predictors of NINV-AR discriminate recurrent HCV-N group from recurrent HCV-I group or recurrent HCV-F group? (ii) Do the best predictors of AR discriminate NINV-NR group from recurrent HCV-N, recurrent HCV-I, or recurrent HCV-F group? (iii) Do the best predictors of AR discriminate NINV-AR group from recurrent HCV-N, recurrent HCV-I or recurrent HCV-F group?

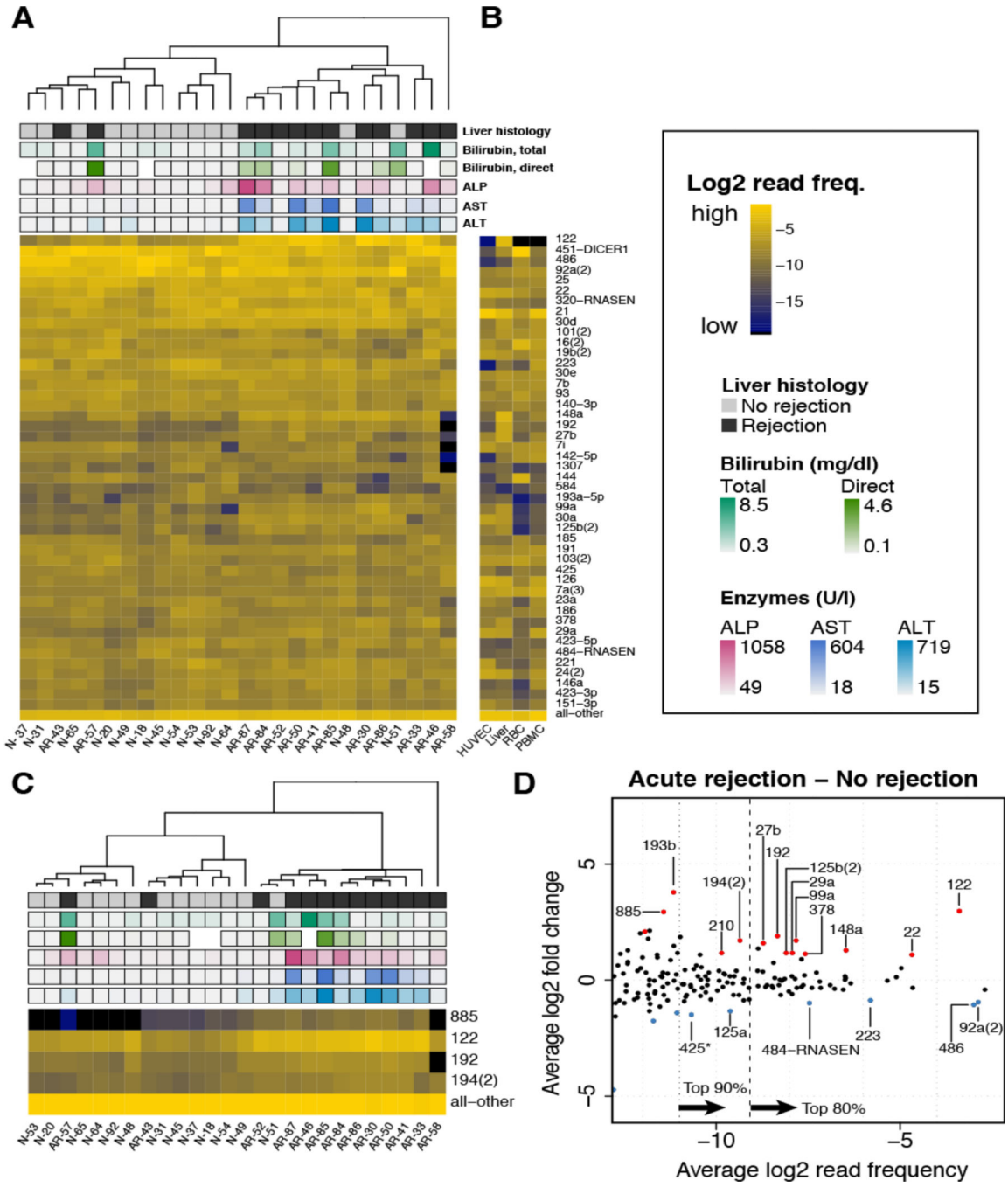

Figure 2. Heatmap of circulating extracellular micro RNAs in sera matched to liver allograft biopsies, micro RNA expression in selected tissues and cells and differential gene abundance analysis: nonimmune nonviral cohort.

A total of 30 sera matched to 30 liver allograft biopsies were processed for small RNA sequencing and 4 of 30 sera (3 sera matched no Rejection biopsies, N-27, N-55, N-56 and 1 serum matched to acute rejection biopsy, AR-44) did not pass quality control thresholds and were excluded from downstream analysis. Unsupervised hierarchical clustering (Euclidean distance, complete linkage) of circulating extracellular micro RNAs showing individual micro RNAs that constitute the top 80% sequencing reads in the remaining 26 of 30 sera

matched to liver allograft biopsies (A); compared to human vascular endothelial cells, liver tissue, red blood cells, and peripheral blood mononuclear cells (B); and of chosen liver-typic micro RNAs (C). Residual micro RNAs are shown as “all-other” at the bottom of each heatmap; samples were clustered by rows and columns, but the row dendrogram is not shown. The inbox indicates the coloring and codes used in panels A-C. MA-plot showing the results of differential gene abundance analysis comparing micro RNAs from the 13 serum samples matched to 13 liver allograft biopsies showing acute rejection with micro RNAs from the 13 serum samples matched to 13 liver allograft biopsies without any rejection changes (no rejection, N) biopsies (D). Micro RNAs in sera from patients with acute rejection compared to sera from patients with no rejection histology are colored red if higher or blue if lower. Micro RNAs on the right side of the 2 vertical dashed lines are composed of 80% or 90% of all sequencing reads across all samples; low abundance micro RNAs further to the left are not shown in this plot. ALP, serum alkaline phosphatase; ALT, serum alanine aminotransferase; AST, serum aspartate aminotransferase; HUVEC, human vascular endothelial cells; PBMC, human peripheral blood mononuclear cells; RBC, human red blood cells.

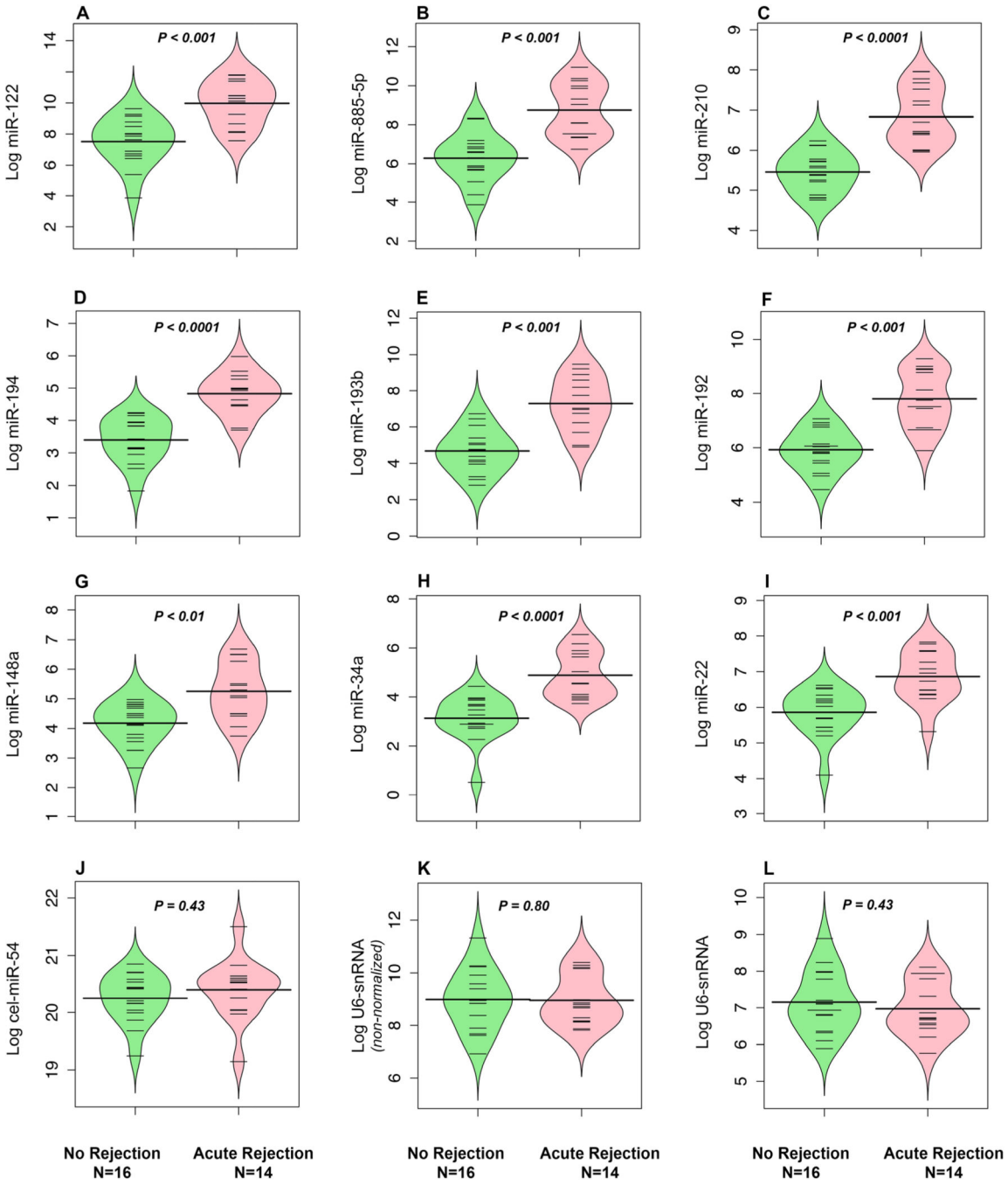

Figure 3. Violin plots of circulating levels of miRNAs in sera matched to liver allograft biopsies: NINV cohort.

Total RNA was isolated from pristine aliquots of 30 sera for absolute quantification of miRNAs using customized real time quantitative polymerase chain reaction assays. The miRNA copy numbers were normalized using the spiked-in cel-miR-54 copy number ($x10^{-8}$) in the same serum sample, and the ratio of miRNA copies to cel-miR-54 copies ($x10^{-8}$) was $\log_e$ transformed prior to data visualization using violin plots and statistical analysis. In the violin plots, the distribution of the ratios in the 16 sera matched to 16 liver allograft biopsies without histological features of acute rejection (No Rejection, in green)

and in the 14 sera matched to 14 acute liver allograft rejection biopsies (Acute Rejection, in pink) is represented by the density shape; the thin black lines show the ratio of messenger RNA copy numbers to cel-miR-54 copy number ($x10^{-8}$) for each serum sample, and the thick black horizontal line crossing the contour of the violin plot show the mean for that group. the mean for each distribution is shown as a thick black horizontal line crossing the contour of the individual violin plot. The *P*-values are based on the Mann-Whitney *U* test comparing the acute rejection group with the no rejection group. miR, microRNA; snRNA, small nuclear RNA.

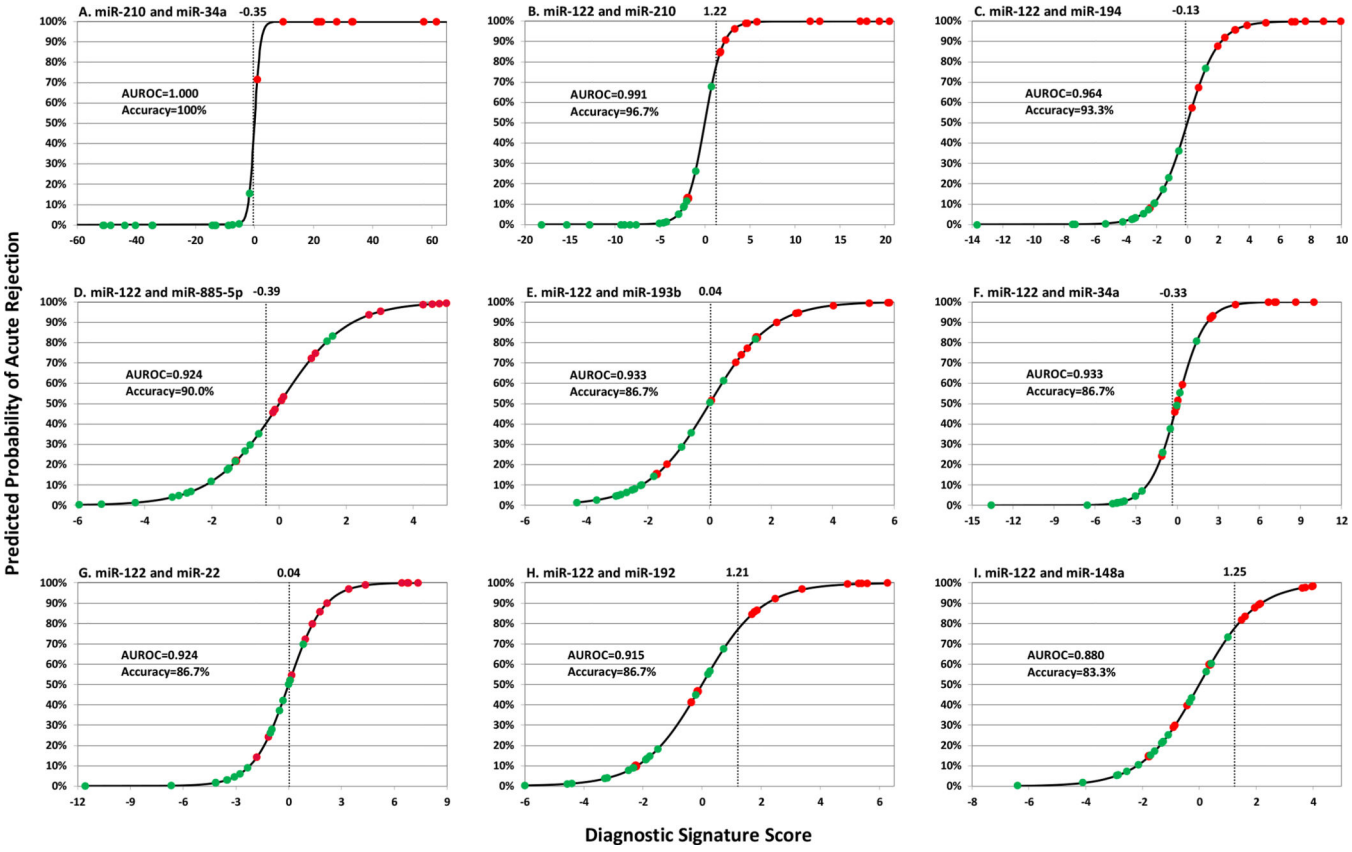

Figure 4. Predicted probability of acute rejection for circulating level of extracellular based statistical models: nonimmune nonviral cohort.

A, Plot shows the predicted probability of acute rejection for given levels of a diagnostic signature based on miR-210 and miR-34a. The y-axis represents the probability of acute rejection. The x-axis represents the diagnostic signature score, which is a linear combination of liver specific miR-210 and miR-34a (normalized by cel-miR-54 ($x10^{-8}$) and $\log_e$ transformed), determined by logistic regression analysis (Table S4). The vertical dotted line represents the cut point of the diagnostic signature score that maximized the combined sensitivity and specificity (Youden's index) to discriminate between sera matched to acute rejection biopsies and sera matched to no rejection biopsies. The value of this cut point is shown at the top of the vertical line. Each serum sample is represented by a colored dot; sera matched to acute rejection biopsies are shown in red and sera matched to no rejection biopsies are shown in green. A comparison of models using Akaike information criterion showed that this miR-210 + miR-34a model is superior to all other 2-miRNA prediction models (Δ Akaike information criterion was ≥ 5.9). The Akaike weight for the combination of miR-210 + miR-34a compared to the 35 other 2-miRNA combinations was 84.0% (Table S4).

B-I, Graphs depict the logistic regression model-based linear combination of miR-122 with each of the 8 informative miRNAs. The y-axis represents the probability of acute rejection. The x-axis represents the diagnostic signature score, which is a linear combination of liver specific miR-122 and each of the other 8 miRNAs (normalized by cel-miR-54 ($x10^{-8}$) and $\log_e$ transformed), determined by logistic regression analysis (Table 4). The vertical

dotted line represents the cut point of the diagnostic signature score that maximized the combined sensitivity and specificity (Youden's index) to discriminate between sera matched to acute rejection biopsies and sera matched to no rejection biopsies. The value of this cut point is shown at the top of the vertical line. In Panels B-I, each serum sample is represented by a colored dot; sera matched to acute rejection biopsies are shown in red and sera matched to no rejection biopsies are shown in green. A comparison of models using Akaike information criterion showed that the miR-122 + miR-210 combination is superior to all other 2-miRNA prediction models that include miR-122 (Δ Akaike information criterion was ≥ 4.5). The Akaike weight for this combination of miR-122 + miR-210 compared to the other 7 combinations that included miR-122, was 88.5% (Table S4). AUROC, area under the receiver operating characteristic curve; miR, micro RNA.

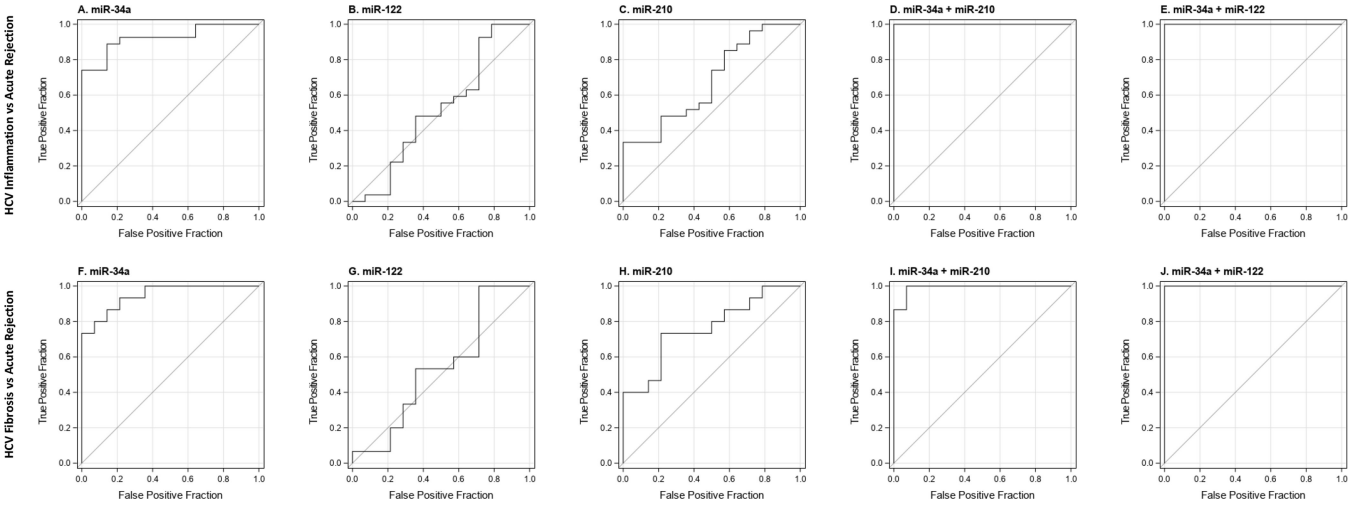

Figure 5. Receiver operating characteristic curve analyses: nonimmune nonviral acute rejection vs recurrent HCV-inflammation and nonimmune nonviral acute rejection vs recurrent-HCV-fibrosis.

Receiver operating characteristic curve analyses portraying the extent to which miR-34a, miR-122, miR-210 and the 2-miRNA combinations distinguish the nonimmune nonviral acute rejection group from the recurrent HCV-inflammation group and from the recurrent-HCV-fibrosis group. For nonimmune nonviral acute rejection vs recurrent HCV-inflammation, the area under the receiver operating characteristic curve (95% CI) for miR-34a was 0.92 (0.84–1.000) (P<0.0001, Figure 5 A); 0.52 (0.31–0.73) for miR-122 (P=0.94, Figure 5B); 0.68 (0.50–85) for miR-210 (P=0.02, Figure 5 C), 1.00 (1.00–1.00) for miR-34a + miR-210 (P=<0.0001, Figure 5 D) and 1.00 (1.00–1.00) for miR-34a + miR-122 (P=<0.0001, Figure 5 E). For nonimmune nonviral acute rejection vs recurrent-HCV-fibrosis, the area under the receiver operating characteristic curve (95% CI) for miR-34a was 0.95 (0.88–1.000) (P <0.0001, Figure 5 F); 0.54 (0.31–0.76) for miR-122 (P=0.74, Figure 5G); 0.76 (0.58–0.94) for miR-210 (P=0.02, Figure 5 H); 0.99 (0.97–1.00) for miR-34a + miR-210 (P<0.0001, Figure 5 I); and 1.00 (1.00–1.00) for miR-34a + miR-122 (P=<0.0001, Figure 5 J). Table 7 shows the Youden's cutpoint, sensitivity, specificity and accuracy for-miR-34a, miR-122, miR-210 and for the 2-miR models, and their logistic regression equations. HCV, hepatitis C virus; miR, micro RNA.

Table 1.

Characteristics of liver allograft recipients: nonimmune nonviral cohort.

Characteristics	Liver allograft biopsy diagnosis		
	Acute rejection biopsy	No rejection biopsy	*P* [a]
Recipient characteristics			
Number of patients [b]	12	15	
Number of serum samples matched to biopsies [c]	14	16	
Age, y, median (min–max)	55 (20–66)	56 (27–69)	0.41
Sex, male / female	7 / 5	11 / 4	0.45
Race, Black / non-Black	1 /11	0 / 15	0.44
Body mass index, kg/m^2, median (min–max)	27.3 (21.3–37.7)	28.4 (16.6–46.1)	0.66
Reason for the live allograft biopsy, for-cause / protocol-specified	12 / 2	1 / 15	<0.0001
Time from transplantation to biopsy, d, median (min–max)	145 (11–905)	378 (20–718)	0.013
Liver function tests			
Serum total bilirubin, mg/dL, median (min–max)	0.95 (0.3–8.5)	0.65 (0.4–4.9)	0.44
Serum direct bilirubin, mg/dL, median (min–max)	0.45 (0.1–4.6)	0.10 (0.1–2.3)	0.04
Serum aspartate aminotransferase, U/L, median (min–max)	146 (18–983)	24 (8–50)	0.0008
Serum alanine aminotransferase, U/L, median (min–max)	260 (22–719)	22 (15–137)	0.0001
Serum alkaline phosphatase, U/L, median (min–max)	281 (75–1058)	90 (49–330)	0.002
Kidney function test			
Serum creatinine, mg/dL, median (min–max)	1.0 (0.6–2.1)	1.3 (0.7–1.8)	0.18
Deceased donor characteristics			
Age, y, median (min–max)	44 (15–73)	46 (22–73)	0.30
Sex, matched / not matched	6 / 6	10 / 5	0.45
Race, matched / not matched	11 / 1	10 / 5	0.18

[a] *P* values based on Mann-Whitney *U* test (with 0.5 continuity correction) for numeric variables or Fisher exact test for dichotomous variables.

[b] 26 unique patients with nonviral nonimmune viral native liver disease (NINV cohort) underwent 30 liver allograft biopsies. Table 1, Row 3 shows 27 patients, since 1 patient who had an initial biopsy classified as acute rejection biopsy had a subsequent biopsy performed 1 year later that was classified as no rejection biopsy and this patient is included in both biopsy groups. Among the 12 patients with 14 acute rejection biopsies, 2 patients had 2 acute rejection biopsies and among 15 patients with 16 no rejection biopsies, 1 patient had 2 no rejection biopsies. Additional patient-specific data, including liver allograft biopsy findings, are provided in Table S1A.

[c] Among the 14 sera matched to 14 acute rejection biopsies from the 12 patients, 12 sera were collected on the same day as the biopsy, 1 serum was collected 1 day after the biopsy and 1 serum was collected 2 days before the biopsy procedure. Among the 16 sera matched to 16 no rejection biopsies from 15 patients, 14 sera were collected on the same day as the biopsy, 1 serum was collected 1 day before the biopsy and 1 serum was collected 7 days before the biopsy procedure.

Table 2.

Relative frequency of circulating miRNAs evaluated by small RNA sequencing of sera matched to acute rejection biopsies or no rejection biopsies: nonimmune nonviral cohort.

miRNA	Relative frequency (%) of miRNAs in sera matched to acute rejection biopsies or no rejection biopsies		miRNA fold change	Nominal *P*	FDR-adjusted *P*
	Acute rejection	No rejection			
122	17.703%	2.232%	↑7.9	4.993E-07	0.0001238
193b	0.085%	0.006%	↑13.6	0.000236617	0.0235894
194(2)	0.244%	0.076%	↑3.2	0.000285356	0.0235894
195	0.003%	0.000%	↑13.0	0.000642122	0.0297413
192	0.511%	0.138%	↑3.7	0.000664913	0.0297413
22	5.581%	2.600%	↑2.1	0.000719548	0.0297413
27b	0.374%	0.124%	↑3.0	0.001441237	0.0496203
99a	0.705%	0.215%	↑3.3	0.001600656	0.0496203
378	0.754%	0.342%	↑2.2	0.001890715	0.0510347
191*	0.001%	0.028%	↓26.5	0.00205785	0.0510347
29a	0.593%	0.265%	↑2.2	0.003572738	0.080549
22*	0.019%	0.002%	↑10.2	0.005402863	0.1116592
450b	0.001%	0.018%	↓18.6	0.007066881	0.1313309
125a	0.076%	0.190%	↓2.5	0.007413842	0.1313309
34a	0.043%	0.010%	↑4.3	0.008762737	0.1361998
210	0.156%	0.070%	↑2.2	0.008787085	0.1361998
484	0.395%	0.788%	↓2.0	0.010224969	0.1411054
125b-2*	0.022%	0.002%	↑9.4	0.010241519	0.1411054
885–5p	0.067%	0.009%	↑7.6	0.011619594	0.1429741
148a	1.667%	0.690%	↑2.4	0.012586277	0.1429741
1468	0.005%	0.001%	↑8.7	0.012718989	0.1429741
425*	0.033%	0.095%	↓2.8	0.013057447	0.1429741
92a(2)	9.651%	18.880%	↓2.0	0.013259697	0.1429741
769	0.027%	0.071%	↓2.7	0.01405606	0.145246
125b(2)	0.527%	0.237%	↑2.2	0.01490957	0.1479029

The relative frequencies of circulating extracellular miRNAs in sera matched to liver allograft biopsies from the nonimmune nonviral cohort are shown. miRNA fold change (ratio of mean frequency in sera matched to nonimmune nonviral acute rejection biopsies to mean frequency in sera matched to nonimmune nonviral no rejection biopsies), nominal *P* value and FDR-adjusted *P* values are shown for each miRNA. Green arrow denotes increased fold change of miRNAs in sera matched to acute rejection biopsies vs sera matched to no rejection biopsies. Red arrow denotes reduced fold change of miRNAs in in sera matched to acute rejection biopsies vs sera matched to no rejection biopsies. The miRNAs are ordered on the basis of nominal *P* value (and FDR-adjusted *P)*. miRNAs with FDR-adjusted $P<0.15$ by both small RNA sequencing and by TaqMan® low density arrays microarray profiling were prioritized for absolute quantification of miRNA copy number using customized real-time quantitative polymerase chain reaction assays. miR nomenclature: numbering of miRNAs is sequential. Canonical miRNAs are generated from hairpin precursors yielding 2 mature sequences. If 1 of the processed molecules is degraded and much less abundant it is called the ‘star’ sequence and indicated by an asterisk. Identical mature sequences processed from distinct precursor sequences are indicated by numbered suffixes and can be conveniently aggregated with the number of aggregated miRNAs given in parentheses. Closely related but not identical mature sequences have letter suffixes.

FDR, false discovery rate; miRNA, micro RNA.

Table 3.

miR-122-based statistical models for the diagnosis of acute rejection in human liver allografts: nonimmune nonviral cohort.

Diagnostic signature	Logistic model equation	AUROC (95%CI)	*P*	Diagnostic signature cut point	Sensitivity (%)	Specificity (%)	Accuracy (%)
miR-122 + miR-210	−63.59 + (1.58*miR-122) + (8.28*miR-210)	0.99 (0.97–1.00)	<0.0001	1.22	93	100	97
miR-122 + miR-194	−24.74 + (1.20*miR-122) + (3.51*miR-194)	0.96 (0.90–1.00)	<0.0001	−0.13	93	94	93
miR-122 + miR-885–5p	−12.63 + (−0.23*miR-122) + (1.96*miR-885–5p)	0.92 (0.83–1.00)	<0.0001	−0.39	93	88	90
miR-122 + miR-193b	−6.13 + (−0.97*miR-122) + (2.46*miR-193b	0.93 (0.85–1.00)	<0.0001	0.04	86	88	87
miR-122 + miR-34a	−16.42 + (0.25*miR-122) + (3.59*miR-34a)	0.93 (0.85–1.00)	<0.0001	−0.33	93	81	87
miR-122 + miR-22	−26.21 + (1.27*miR-122) + (2.38*miR-22)	0.92 (0.83–1.00)	<0.0001	0.04	86	88	87
miR-122 + miR-192	−17.00 + (0.09*miR-122) + (2.40*miR-192)	0.92 (0.82–1.00)	<0.0001	1.21	71	100	87
miR-122 + miR-148a	−11.76 + (1.14*miR-122) + (0.35*miR-148a)	0.88 (0.76–1.00)	<0.0001	1.25	64	100	83

Each diagnostic signature is a statistical model developed as a linear combination of liver specific miR-122 and 1 of the other 8 miRNAs based on the parameter estimates from a logistic regression analysis predicting nonimmune nonviral acute rejection biopsy vs. nonimmune nonviral no rejection biopsy. In this analysis, $\log_e$ ratios of miRNA copy numbers to cel-miR-54 copy number ($x10^{-8}$) in sera were used as predictors. The logistic regression equation shows the intercept, the slope (coefficient) of miR-122 ($\log_e$ ratio of miR-122 copy number to cel-miR-54 copy number [$x10^{-8}$]) and the slope (coefficient) of the second miRNAs ($\log_e$ ratio of miRNA copy number to cel-miR-54 copy number [$x10^{-8}$]). The intercept and slopes have no intrinsic units of measurement. The AUROC is the area under the ROC curve for the logistic (diagnostic signature) model. The diagnostic signature cut point is the value that maximizes the combined sensitivity and specificity (Youden's index) for discriminating biopsy specimens showing acute rejection from those not showing acute rejection in the liver allograft biopsies.

AUROC, area under the receiver operating characteristic curve; miR, micro RNA.

Table 4.

Bootstrap analysis with 10 000 replication of 2-miRNA models diagnostic of acute rejection in human liver allografts: nonimmune nonviral cohort.

Model	Estimated AUROC (95% CI)	Bootstrap standard error	Bias	Bias-corrected 95% CI
miR-210 + miR-34a	1.000 (1.000–1.000)	0.000	0.000	1.000–1.000
miR-122 + miR-210	0.991 (0.970–1.000)	0.014	-0.355	0.929–1.000

Logistic regression analyses identified that the 2-miRNA model of miR-210 + miR-34a with the following parameters −291.3+ (40.66*miR-210) + (12.88*mIR-34A) was the best model among 36 2-miRNA combinations and discriminated the nonimmune nonviral acute rejection group from the nonimmune nonviral no rejection group with an AUROC of 1.0. Internal validation by bootstrap resampling necessarily yielded a bias-corrected 95% CI of 1.00–1.00. A linear combination of liver specific miR-122 + miR-210 with the following parameters −63.59 + (1.58*miR-122) + (8.28*miR-210) was the best model among the 8 models that included miR-122 with an AUROC of 0.991. Internal validation by bootstrap resampling yielded a bias-corrected 95% CI of 0.929–1.000. In both analyses, $\log_e$ ratios of miRNA copy numbers to cel-miR-54 copy number ($x10^{-8}$) in sera were used as predictors.

AUROC, area under the receiver operating characteristic curve; miR, micro RNA.

Table 5.

Characteristics of liver allograft recipients: recurrent HCV cohort.

Characteristics		Liver allograft biopsy diagnosis					
	Recurrent HCV-normal (HCV-N)	Recurrent HCV-inflammation (HCV-I)	Recurrent HCV-fibrosis (HCV-F)	*P* [a]	*P* [b] (Pairwise comparison)		
					HCV-N vs HCV-I	HCV-N vs HCV-F	HCV-I vs HCV-F
Recipient characteristics							
Number of patients [c]	13	23	12				
Number of serum samples matched to biopsies [d]	19	27	15				
Age, y, median (min–max)	55 (42–67)	55 (35–62)	54 (42–60)	0.74	0.74	0.66	0.47
Sex, male / female	12 / 1	21 / 2	10 / 2	0.71	0.99	0.59	0.59
Race, Black / non-Black	4 / 9	9 / 14	3 / 9	0.68	0.73	0.99	0.48
Body mass index, kg/m^2, median (min–max)	29.8 (20.1–38.7)	29.7 (22.2–37.2)	28.1 (19.2–36.1)	0.42	0.98	0.37	0.19
Reason for the live allograft biopsy, for-cause / protocol	9 / 10	9 / 18	3 / 12	0.25	0.37	0.15	0.48
Time from transplantation to biopsy, d, median (min–max)	199 (11–747)	232 (42–1392)	401 (179–1299)	0.0015	0.31	0.0003	0.0046
Liver function tests							
Serum total bilirubin, mg/dL, median (min–max)	0.8 (0.3–14.7)	1.0 (0.5–5.5)	1.0 (0.5–3.5)	0.29	0.12	0.29	0.87
Serum direct bilirubin, mg/dL, median (min–max)	0.3 (0.0–14.2)	0.3 (0.2–4.7)	0.5 (0.1–2.2)	0.23	0.15	0.17	0.61
Serum aspartate aminotransferase, U/L, median (min–max)	36 (18–524)	154 (35–844)	125 (22–419)	0.0032	0.001	0.0109	0.76
Serum alanine aminotransferase, U/L, median (min–max)	53 (21–328)	129 (30–1404)	119 (41–386)	0.02	0.0058	0.09	0.48
Serum alkaline phosphatase, U/L, median (min–max)	114 (65–1743)	135 (45–918)	144 (45–268)	0.80	0.49	0.99	0.74
Kidney function test							
Serum creatinine, mg/dL, median (min–max)	1.4 (0.7–4.2)	1.2 (0.8–2.1)	1.1 (0.8–2.9)	0.24	0.45	0.08	0.30
Deceased donor characteristics							
Age, y, median (min–max)	37 (18–67)	44 (16–73)	33 (9–73)	0.83	0.61	0.97	0.64
Sex, matched / not matched	10 / 3	15 / 8	8 / 4	0.76	0.71	0.67	0.99
Race, matched / not matched	6 / 7	11 / 12	8 / 4	0.50	0.99	0.43	0.48

[a] *P* values based on Mann-Whitney *U* test (with 0.5 continuity correction) for numeric variables or Fisher exact test for dichotomous variables.

[b] *P* values based on Mann-Whitney *U* test (with 0.5 continuity correction) for numeric variables or Fisher exact test for dichotomous variables.

[c] Forty-one unique patients with recurrent HCV underwent 61 liver allograft biopsies. Table 6, Row 3 shows 48 patients since 3 patients with an initial HCV normal biopsy had subsequent biopsies 5, 6, and 39 months later that were classified as HCV inflammation and these 3 patients are included under the recurrent HCV inflammation group as well, and 1 patient with an initial recurrent HCV normal biopsy had a subsequent biopsy 7 months later that was classified as recurrent HCV fibrosis and this patient is included under the HCV fibrosis group as well. Among the recurrent HCV inflammation biopsy group, 3 patients had an initial biopsy classified as recurrent HCV inflammation and subsequent biopsies 3, 5, or 6 months later that was classified as recurrent HCV fibrosis and these 3 patients are included under recurrent HCV-F group as well. Among the 12 patients with recurrent HCV fibrosis biopsies, 6 patients had 1 recurrent HCV fibrosis biopsy each and 3 patients had 2 R-HCV fibrosis biopsies each. Additional patient-specific data, including liver allograft biopsy findings, are provided in Table S1B.

[d] miR-34a, miR-122 and miR-210 were quantified in 61 sera matched to 61 liver allograft biopsies using customized real-time quantitative polymerase chain reaction assays. These 3 micro RNAs, diagnostic of nonimmune nonviral acute rejection and included in the acute rejection diagnostic models, were prioritized for analysis in sera matched to liver allograft biopsies from the patients with recurrent HCV. Among the 19 sera matched to 19 recurrent HCV normal biopsies from 13 patients, 12 sera were collected on the same day as the biopsy, 1 serum was collected 2 days after the biopsy, 5 sera were collected 1 day before the biopsy and 1 serum was collected 2 days before the biopsy procedure. Among the 27 sera matched to 27 recurrent HCV inflammation biopsies from 23 patients, 23 sera were collected on the same day as the biopsy, 1 serum was collected 1 day after the biopsy, 2 sera were collected 2 days before the biopsy and 1 serum was collected 3 days before the biopsy procedure. Among the 15 sera matched to 15 recurrent HCV fibrosis biopsies from 12 patients, 12 sera were collected on the same day as the biopsy, and 3 sera were collected 1 day before the biopsy procedure.

HCV, hepatitis C virus; HCV-F, HCV-fibrosis; HCV-I, HCV-inflammation; HCV-N, HCV-normal.

Table 6.

Circulating levels of miRNAs in nonimmune nonviral cohort and recurrent HCV cohort.

miRNA	NR sera (N=16)	AR sera (N=14)	HCV-N sera (N=19)	HCV-I sera (N=27)	HCV-F sera (N=15)		*P* NR vs	*P* AR vs	*P* HCV-N vs	*P* HCV-I vs
cel-miR-54	20.311 (20.015, 20.563)	20.530 (20.045, 20.606)	20.061 (19.779, 20.750)	20.081 (19.743, 20.454)	20.021 (19.797, 20.416)	AR HCV-N HCV-I HCV-F	0.3731 0.7509 0.3562 0.5276	0.3042 0.0863 0.2158	0.6324 0.7595	0.9506
miR-34A	3.098 (2.831, 3.782)	4.566 (4.023, 5.758)	6.355 (5.324, 7.247)	7.407 (6.130, 7.918)	7.345 (6.435, 8.104)	AR HCV-N HCV-I HCV-F	<0.0001 <0.0001 <0.0001 <0.0001	0.0006 <.0001 <.0001	0.0142 0.0095	0.7370
miR-122	7.751 (6.667, 8.635)	10.208 (8.657, 11.396)	9.357 (8.783, 10.118)	10.203 (8.703, 11.010)	9.933 (8.679, 10.769)	AR HCV-N HCV-I HCV-F	<0.0001 0.0004 <0.0001 <0.0001	0.0626 0.9407 0.7380	0.0195 0.0777	0.7231
miR-210	5.487 (5.050, 5.753)	6.585 (6.389, 7.522)	5.821 (5.336, 6.347)	6.425 (5.374, 6.717)	6.013 (5.703, 6.483)	AR HCV-N HCV-I HCV-F	<0.0001 0.4318 0.0049 0.0018	0.0002 0.0159 0.0157	0.0781 0.0992	0.9824

Median (lower, upper quartiles) of $\log_e$-transformed cel-miR-54 copies (spiked-in-control) and $\log_e$-transformed ratios of serum miRNA copies to serum cel-miR-54 ($x10^{-8}$) copies in 16 sera matched to 16 NR biopsies from the nonimmune nonviral cohort (NR Sera), 14 sera matched to 14 acute rejection biopsies from the NINV-AR cohort (AR sera), 19 sera matched to 19 biopsies from the recurrent HCV cohort with biopsies without intragraft inflammation or fibrosis and classified as normal biopsies (recurrent HCV-N sera), 27 sera matched to 27 biopsies from the recurrent HCV cohort with biopsies with intragraft inflammation (recurrent HCV-I sera) and 15 sera with matched to 15 biopsies from the recurrent HCV cohort with biopsies with intragraft fibrosis (recurrent HCV-F sera). These 3 miRNAs diagnostic of nonimmune nonviral-AR (vs nonimmune nonviral-NR) and included in the best AR diagnostic models were therefore prioritized for analysis in sera matched to liver allograft biopsies from the patients with recurrent HCV. *P*-values are based on the log-likelihood ratio chi-square test comparing nested logistic regression models. The polymerase chain reaction for each sample was set up in duplicate as 20μl reaction volume using 1μl 20x TaqMan miRNA-specific primer and probe, 1.5μl of preamplified complementary DNA (at 1:20 dilution), 10μl of TaqMan Universal polymerase chain reaction Master mix and 7.5μl of nuclease-free water. A standard curve was established for each polymerase chain reaction assay using polymerase chain reaction-generated 73-bp mouse Bak amplicon developed in the Gene Expression Monitoring Core.

AR, acute rejection; HCV, hepatitis C virus; HCV-F, HCV fibrosis; HCV-I, HCV inflammation; HCV-N, HCV normal; miRNA, micro RNA; NR, no rejection.

Table 7A.

Differential diagnosis of nonimmune nonviral acute rejection biopsy group vs recurrent hepatitis C virus inflammation biopsy group.

Predictor / diagnostic signature	Logistic model equation	AUROC (95% CI)	*P*	Diagnostic signature cut point	Sensitivity (%)	Specificity (%)	Accuracy (%)
miR-34a	- - -	0.92 (0.84–1.00)	<0.0001	5.91	86	89	88
miR-122	- - -	0.52 (0.31–0.73)	0.94	11.50	21	96	73
miR-210	- - -	0.68 (0.50–0.85)	0.02	5.88	100	33	56
miR-34a + miR-210	−21.45 + (−26.29*miR-34a) + (29.82*miR-210)	1.00 (1.00–1.00)	<0.0001	0.06	100	100	100
miR-34a + miR-122	32.56 + (13.59*miR-34a) + (−11.76*miR-122)	1.00 (1.00–1.00)	<0.0001	4.94	100	100	100

Table 7B.

Differential diagnosis of nonimmune nonviral acute rejection biopsy group vs recurrent hepatitis C virus fibrosis biopsy group.

Predictor / diagnostic signature	Logistic model equation	AUROC (95% CI)	*P*	Diagnostic signature cut point	Sensitivity (%)	Specificity (%)	Accuracy (%)
miR-34a	- - -	0.95 (0.88–1.00)	<0.0001	6.57	100	73	86
miR-122	- - -	0.54 (0.31–0.76)	0.74	11.26	29	100	66
miR-210	- - -	0.76 (0.58–0.94)	0.015	6.37	79	73	76
miR-34a + miR-122	32.56 + (13.59*miR-34a) + (−11.76*miR-122)	1.00 (1.00–1.00)	<0.0001	0.26	100	100	100
miR-34a + miR-210	−21.45 + (−26.29*miR-34a) + (29.82*miR-210)	0.99 (0.97–1.00)	<0.0001	28.06	93	100	97

Measures summarizing the ability of 3 individual miRNAs diagnostic of nonimmune nonviral acute rejection and the best miRNA diagnostic signatures to discriminate 14 sera matched to 14 nonimmune nonviral acute rejection biopsies from either 27 sera matched to 27 biopsies classified as recurrent hepatitis C virus inflammation or 15 sera matched to 15 biopsies classified as recurrent hepatitis C virus fibrosis. Each miRNA measure is the $\log_e$-transformed ratio of the miRNA copy number to the cel-miR-54 copy number ($x10^{-8}$) in sera. The diagnostic signatures are a linear combination of 2 miRNAs based on the parameter estimates from logistic regression analyses predicting nonimmune nonviral acute rejection vs recurrent hepatitis C virus inflammation and nonimmune nonviral acute rejection vs recurrent hepatitis C virus fibrosis. Each logistic model equation shows the intercept and the slopes (coefficients) of the 2 $\log_e$–transformed ratios of the specified miRNA copy number to cel-miR-54 copy number ($x10^{-8}$). The intercept and slopes have no intrinsic units of measurement. The AUROC is the area under the ROC curve for the predictor/diagnostic signature. *P*-values are based on the log-likelihood ratio chi-square test comparing nested logistic regression models. The cut point is the value that maximizes the combined sensitivity and specificity (Youden's index) for discriminating biopsy specimens showing acute rejection from those showing recurrent hepatitis C virus-inflammation (Panel A) or recurrent hepatitis C virus-fibrosis (Panel B) in the liver allograft biopsies. For analyses discriminating nonimmune nonviral acute rejection vs recurrent hepatitis C virus-inflammation (Panel A), the Akaike information criterion was 4.52 and Akaike weight was 61.8% for miR-34a + miR-210 and the Akaike information criterion was 5.48 and Akaike weight was 38.2% for miR-34a + miR-122. Based on this criteria, miR-34a +miR-210 best discriminated nonimmune nonviral acute rejection from recurrent hepatitis C virus-inflammation. For analyses discriminating nonimmune nonviral acute rejection vs recurrent hepatitis C virus fibrosis (Panel B), the Akaike information criterion was 4.03 and Akaike weight was 98.7% for miR-34a + miR-122 and the Akaike information criterion was 12.69 and Akaike weight was 1.3% for miR-34a + miR-210. Based on this criteria, miR-34a +miR-122 best discriminated nonimmune nonviral acute rejection from recurrent hepatitis C virus-fibrosis (Table S6).

AUROC, area under the receiver operating characteristic curve; miR, micro RNA.